Monodentate function of the 4,4′-bipyridine that systematically occurs in the 4-sulfobenzoate manganese(II) complexes: syntheses, crystal structures, and properties

Li-Ping Zhang and Long-Guan Zhu*

Received 4th August 2006, Accepted 21st September 2006
First published as an Advance Article on the web 28th September 2006
DOI: 10.1039/b611300a

In this presentation, three topologically diverse complexes based on the Mn^{2+}/4-sulfobenzoate/4,4′-bipyridine system, $[Mn(4,4'\text{-bipy})_2(H_2O)_4](Hsb)$ (**1**), $[Mn(4,4'\text{-bipy})_2(H_2O)_4](sb)(4H_2O)$ (**2**), and $\{[Mn(4,4'\text{-bipy})(sb)(H_2O)_3](2H_2O)\}_n$ (**3**) [4,4′-bipy = 4,4′-bipyridine; sb = 4-sulfobenzoate dianion], have been prepared and characterized by single-crystal X-ray analyses, elemental analyses, IR spectra, TG analyses, and photoluminescence studies. The structures of complexes **1** and **2** are cation–anion species whereas complex **3** is a 1-D polymer. In all three complexes 4,4′-bipyridine ligands feature a monodentate coordination mode and the uncoordinated nitrogen donor of each 4,4′-bipyridine engages in the intermolecular hydrogen bonding, which blocks the metal–metal bridging by 4,4′-bipyridine. In contrast to monodentate 4,4′-bipyridine-containing complexes occasionally reported in the literature, the monodentate function for 4,4′-bipyridine ligands in complexes **1–3** systematically occurs, suggesting the sulfonate group can adjust the competitive coordination between the carboxylate and 4,4′-bipyridine ligands. Extensive hydrogen-bonding interactions including hydrogen-bonded 4,4′-bipyridine in these three complexes control their crystal packings and give rise to 3-D extended supramolecular architectures.

Introduction

In the past decade, a large number of one-, two-, and three-dimensional (1-D, 2-D and 3-D) polymeric complexes have been prepared by 1,4-benzenedicarboxylate (bdc) and/or 4,4′-bipyridine for potential applications as function materials, such as catalysis, magnetism, chemical sensor, and gas absorbent.[1–6] In the process of pursuing excellent functional metal–organic framework materials, systematic tuning of bdc-like complexes has produced numerous extended networks with specific properties as a result of the versatile coordination modes of carboxylates, for example, $Zn_4O(cbdc)_3$ (H_2cbdc = cyclobutyl-1,4-benzenedicarboxylic acid) material has a higher methane storage capacity than that of $Zn_4O(bdc)_3$, although the latter has a larger pore volume.[7] For this reason, we also have conducted a similar fine-tuning exploration to expand functional polymeric materials using different ditopic ligand, a new aromatic ligand with the combination of carboxyl- and sulfonyl-4-sulfobenzoate (sb). The reaction of zinc sulfate with a combination of sb and 4,4′-bipyridine under hydrothermal conditions, unexpectedly, led to a monodentate 4,4′-bipyridine complex.[8] In contrast, however, there is no example of monodentate 4,4′-bipyridine mode in the complexes with both coordinated bdc and 4,4′-bipyridine ligands. Several coordination modes or existing forms of the 4,4′-bipyridine in all previously reported 4,4′-bipyridine-containing metal complexes are summarized below: (i) popular or normal mode, *i.e.* bridging mode in polymeric complexes;[9–14] (ii) dimeric linker serving as only a short bridge;[15–17] (iii) unidentate mode;[18–22] and (iv) protonated mode.[23–26] The first monodentate 4,4′-bipyridine complex confirmed by single-crystal X-ray analysis was prepared by Haim and co-workers in 1978.[18] Since then such complexes have continuously been reported, but these complexes have been synthesized occasionally and investigations on monodentate 4,4′-bipyridine complexes are still limited. Following the successful synthesis of zinc/sb system with monodentate 4,4′-bipyridine, the manganese(II) salt was selected to expand the family of sb complexes. Here, we report syntheses, crystal structures, and properties of a series of complexes favorably incorporating monodentate 4,4′-bipyridine.

Department of Chemistry, Zhejiang University, Hangzhou 310027, People's Republic of China. E-mail: chezlg@zju.edu.cn

Experimental

All starting materials were commercially obtained from Acros Organics and used without further purification. Elemental analyses (C, H, and N) were performed on a Perkin-Elmer 1110 analyzer. IR spectra were recorded on a Nicolet Nexus 470 infrared spectrophotometer in the range of 400–4000 cm^{-1} using KBr pellets. Thermogravimetric analyses were carried out using a Delta Series TG SDT Q600 in nitrogen atmosphere at a heating rate of 10 °C min^{-1} in the temperature range 25 to 800 °C using aluminium crucibles. The photoluminescence study was carried out on a powdered sample in the solid state at room temperature using Hitachi 850 spectrometer. X-Ray powder diffraction (XRPD) data were collected on a Rigaku D/max-3B by using Cu Kα radiation.

Synthesis

Synthesis of $[Mn(4,4'\text{-bipy})_2(H_2O)_4](Hsb)_2$ (1). A mixture of $MnSO_4{\cdot}H_2O$ (0.085 g, 0.5 mmol), potassium hydrogen 4-sulfobenzoate (0.120 g, 0.5 mmol), 4,4′-bipyridine (0.039 g, 0.5 mmol), and water (15 mL) was heated in a 30 mL Teflon-lined stainless steel reactor at 150 °C for 24 h. After cooling the autoclave to room temperature, a light yellow solution was obtained, then the resulting solution was put aside to slowly evaporate for three months. Pale yellow block-shaped crystals were formed and filtered. Crystals were washed with water and ethanol. Yield: 34% based on Mn atom. IR (KBr, cm^{-1}): 3366m, 1702m, 1604s, 1491w, 1410m, 1306m, 1281s, 1240s, 1221s, 1179s, 1132m, 1112s, 1061m, 1036, 1007s, 865w, 806s, 772m, 721s, 696m, 634s, 566w, 511w. Calc. for $C_{34}H_{34}MnN_4O_{10}S_2$: C, 48.52%; H, 4.07%; N, 6.66%. Found: C, 48.58%; H, 3.83%; N, 6.72%.

Synthesis of $[Mn(4,4'\text{-bipy})_2(H_2O)_4](sb)(4H_2O)$ (2). Manganese(II) acetate tetrahydrate (0.063 g, 0.25 mmol) and potassium hydrogen 4-sulfobenzoate (0.060 g, 0.25 mmol) were mixed in water (20 mL). To this solution was slowly added 4,4′-bipyridine (0.02 g, 0.25 mmol) with stirring until the 4,4′-bipyridine has completely dissolved. The resulting solution was left to stand for one week at room temperature. After this period, colorless prism-shaped crystals were obtained and collected by filtration. Crystals were washed with water and ethanol. Yield: 38% based on Mn atom. IR (KBr, cm^{-1}): 3396s, 1599s, 1536s, 1491w, 1413s, 1379s, 1210s, 1182s, 1140w, 1115m, 1066m, 1031s, 1005s, 808s, 732s, 703m, 642m, 624s, 570w, 470w. Calc. for $C_{27}H_{36}MnN_4O_{13}S$: C, 45.57%; H, 5.10%; N, 7.87%. Found: C, 45.56%; H, 4.97%; N, 7.84%.

Synthesis of $\{[Mn(sb)(4,4'\text{-bipy})(H_2O)_3](H_2O)_2\}_n$ (3). This complex was prepared similarly to **1** except for the use of $Mn(CH_3COO)_2{\cdot}4H_2O$ (0.125 g, 0.5 mmol) instead of $MnSO_4{\cdot}H_2O$. The resulting solution was set aside and allowed to slowly evaporate for one week. Colorless prism-shaped crystals were filtered and washed with water and ethanol. Yield: 71% based on Mn atom. IR (KBr, cm^{-1}): 3341s, 1600s, 1533m, 1404s, 1213s, 1180s, 1116s, 1038s, 1008s, 812s, 782w, 733s, 698w, 627m, 492m. Calc. for $C_{17}H_{22}MnN_2O_{10}S$: C, 40.73%; H, 4.42%; N, 5.59%. Found: C, 40.85%; H, 4.39%; N, 5.58%.

Crystallography

Suitable crystals directly grown from the reaction media for **1–3** were used for the structure determinations. All measurements were performed with a Brucker SMART diffractometer equipped with a CCD area detector. The data were integrated by use of the SAINT program,[27] with the intensities corrected for Lorentz factor polarization and absorption. The structures were solved by direct methods and successive Fourier syntheses. Full-matrix least squares refinements on F^2 were carried out using SHELXL-97 package.[28] All non-hydrogen atoms were anisotropically refined. Hydrogen atoms on carbon atoms were placed in idealized positions and refined as riding atoms, with C–H = 0.93 Å and $U_{iso}(H) = 1.2U_{eq}(C)$. H atom of the carboxyl group in **1** was geometrically calculated and refined as riding atom with O–H = 0.82 Å and $U_{iso}(H) = 1.2U_{eq}(O)$. Other H atoms bound to oxygen atoms were located in difference Fourier maps and refined with distance restraints of O–H = 0.85(1) Å and fixed isotropic displacement parameter of $U_{iso}(H)$ = 0.08 $Å^2$. All the programs used are included in the WinGX Suite version 1.70.[29] Crystal data and structure refinements for **1–3** are listed in Table 1.

Table 1 Crystal data and details of structural determination of complexes **1**, **2**, and **3**

Complex	**1**	**2**	**3**
Formula	$C_{34}H_{34}MnN_4O_{10}S_2$	$C_{27}H_{36}MnN_4O_{13}S$	$C_{17}H_{22}MnN_2O_{10}S$
M_r	841.7	711.6	501.37
Crystal color, shape	Light yellow, block	Colorless, prism	Colorless, prism
Crystal size/mm	0.25 × 0.29 × 0.31	0.08 × 0.15 × 0.15	0.35 × 0.39 × 0.44
Space group	Triclinic/$P\bar{1}$	Monoclinic/$P2_1$	Monoclinic/$P2_1$
a/Å	7.5821(7)	7.1234(5)	11.7049(7)
b/Å	7.7098(7)	18.3038(14)	7.2824(4)
c/Å	16.7833(16)	12.4646(9)	13.4553(8)
α/°	92.261(2)	90	90
β/°	93.430(2)	99.972(1)	114.163(1)
γ/°	110.970(1)	90	90
V/$Å^3$	912.52(5)	1600.65(4)	1046.44(5)
Z	1	2	2
D/g cm^{-3}	1.53	1.48	1.59
T/K	293 ± 2	293 ± 2	293 ± 2
μ/mm^{-1}	0.551	0.548	0.788
Measured reflections	6615	8466	6184
Unique reflections	3177	5038	3603
Observed reflections	2906	4396	3586
$F(000)$	435	742	518
$R1$ and $wR2$ ($I > 2\sigma(I)$)	0.059, 0.158	0.050, 0.089	0.035, 0.085
$R1$ and $wR2$ (all data)	0.065, 0.169	0.060, 0.093	0.035, 0.085
Number of variables	262	464	311
Goodness of fit (GOF)	1.103	1.041	1.121
Largest difference peak and hole/e $Å^{-3}$	0.594, −0.445	0.377, −0.375	0.331, −0.329

Results and discussion

Synthesis

In the formation of complexes with compositional and structural diversity based on the same reactants, reaction temperature, solvent, pH, molar ratio, and synthesis method largely influence the final products. In this presentation, to eliminate the complicated combination ratio of reactants, the ratio of Mn^{2+} : sb : 4,4′-bipy was fixed in 1 : 1 : 1. Complexes **1** and **3** were synthesized by a two-step procedure which is a combination of hydrothermal reaction and subsequent solution evaporation, whereas complex **2** was prepared by the typical mixed-solution method. Initially, we prepared complex **1** by use of manganese(II) sulfate. When manganese(II) acetate instead of $MnSO_4$ under similar procedure as in **1**, complex **3** was formed. It is well known that the sulfate anion is more difficult than acetate as a leaving ligand, therefore the structure of complex **3** is formed by infinite 1-D chain where Mn^{2+} centres are linked by sb bridges compared to the non-coordination of sb or Hsb in **1** and **2**. On the other hand, acetate salt can be used to deprotonate the function group of the carboxylic acid, thus in complex **3** the sb is fully deprotonated whereas in complex **1** the sb is only partly deprotonated. Further exploration of the $Mn(CH_3COO)_2$/sb/4,4′-bipy system under moderate conditions generated a new species, complex **2**.

IR spectra

The IR spectrum of complex **1** displays an absorption peak at 1702 cm^{-1}, which suggests that the carboxyl group is not deprotonated, whereas there is no any such peak in complexes **2** and **3**. All three complexes exhibit broad absorption bands in the water-stretching region (3440–3500 cm^{-1}). The wagging vibration of the coordinated water molecule is observed at 566 cm^{-1} for **1**, 570 cm^{-1} for **2**, and 571 cm^{-1} for **3**, respectively. According to ref. 30 monodentate 4,4′-bipyridine typically displays four characteristic peaks at about 1589, 1402, 1215, and 800 cm^{-1}, and these peaks can be clearly recognized at 1604, 1410, 1221, and 806 for **1**, 1599, 1413, 1211, and 808 cm^{-1} for **2**, and 1600, 1404, 1213, and 812 cm^{-1} for **3**, respectively, suggesting that these three complexes are incorporated by monodentate 4,4′-bipyridine ligands. The coordinated and uncoordinated sb ligands are difficult to recognize from the IR spectra because extensive hydrogen bonds occur and ν_s(COO) peak is superimposed by 4,4′-bipyridine absorptions. Despite these difficulties, SO_3 group characteristic peaks are observed. The characteristic vibrations of SO_3^- are at 1179, 1036, and 1007 cm^{-1} in **1**, 1182, 1031, and 1005 cm^{-1} in **2**, and 1180, 1038, and 1008 cm^{-1} in **3** for $\nu_{as}SO_3$, respectively.

Descriptions of crystal structures

Complexes **1** and **2** are all cation–anion species, which made up cations, anions, and lattice water molecules (Fig. 1 and 2) and their powder X-ray patterns are shown in Fig. 3 and 4. The simulated powder patterns for complexes **1** and **2** calculated from the CIFs by Mercury (version 1.3) coincide with the experimental XRPD patterns (Fig. 5 and 6, the positions of the peaks are the same but the strength of some peaks is somewhat changed). Both complexes **1** and **2** contain a $[Mn(4,4'\text{-bipy})_2(H_2O)_4]^{2+}$ (Mn : 4,4′-bipy = 1 : 2) cation in which the coordination environment of the Mn(II) atom is an octahedral geometry, and in **1** the Mn(II) atom lies on an inversion centre (selected bond lengths and angles for complex

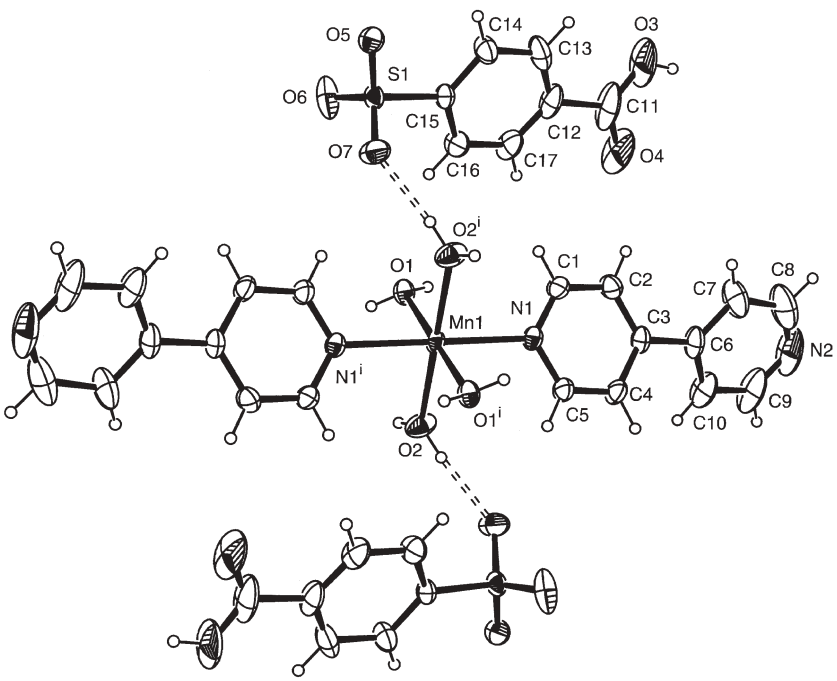

Fig. 1 View of the molecular structure of complex **1**, with 40% probability displacement ellipsoids. Hydrogen bonds are shown as dashed lines. [Symmetry code (i): $-x + 2$, $-y + 2$, $1 - z$.]

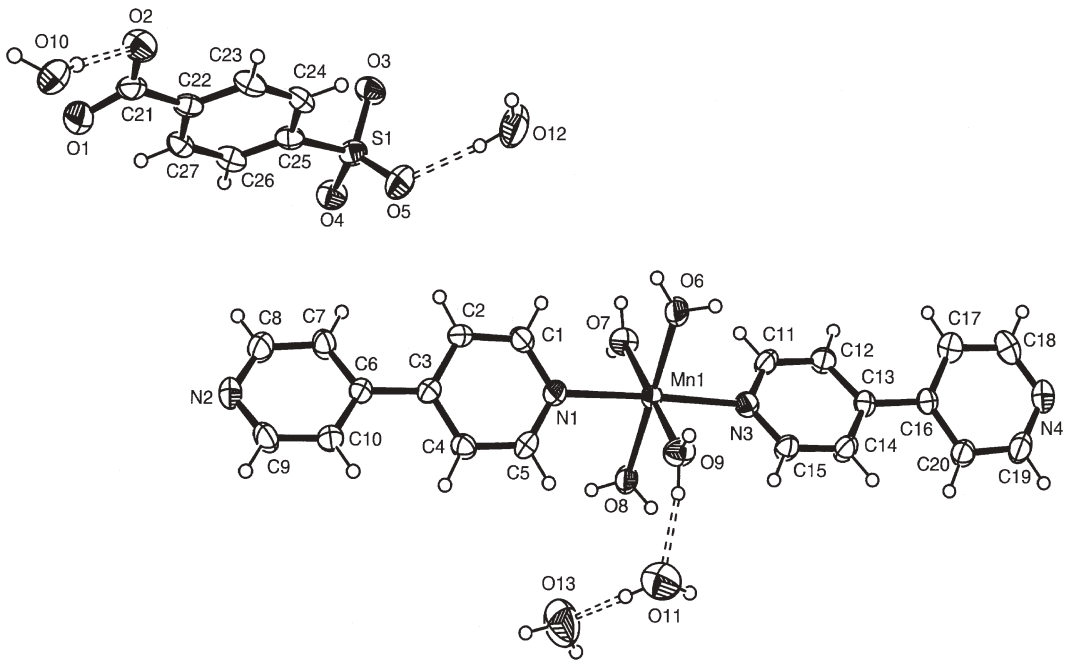

Fig. 2 The molecular structure of complex **2**, with 40% probability displacement ellipsoids. Hydrogen bonds are shown as dashed lines.

1 are given in Table 2). It is interesting that there are some differences in complexes **1** and **2** for their bond lengths. In **2** Mn–N distances [2.270(3)–2.285(3) Å] are slightly longer than those in **2** [2.250(3) Å], whereas Mn–O [2.152(3)–2.159(2) Å] except Mn1–O9 is shorter than those in **1** [2.182(3)–2.199(3) Å]. Moreover, the anions in **1** and **2** are very different, in **1** 4-sulfobenzoate is singly deprotonated whereas in **2** it is fully deprotonated. To our knowledge, only four complexes containing $[Mn(4,4'\text{-bipy})_2(H_2O)_4]^{2+}$ species have been reported, $[Mn(4,4'\text{-bipy})_2(H_2O)_4](ClO_4)_2(4,4'\text{-bipy})_4$

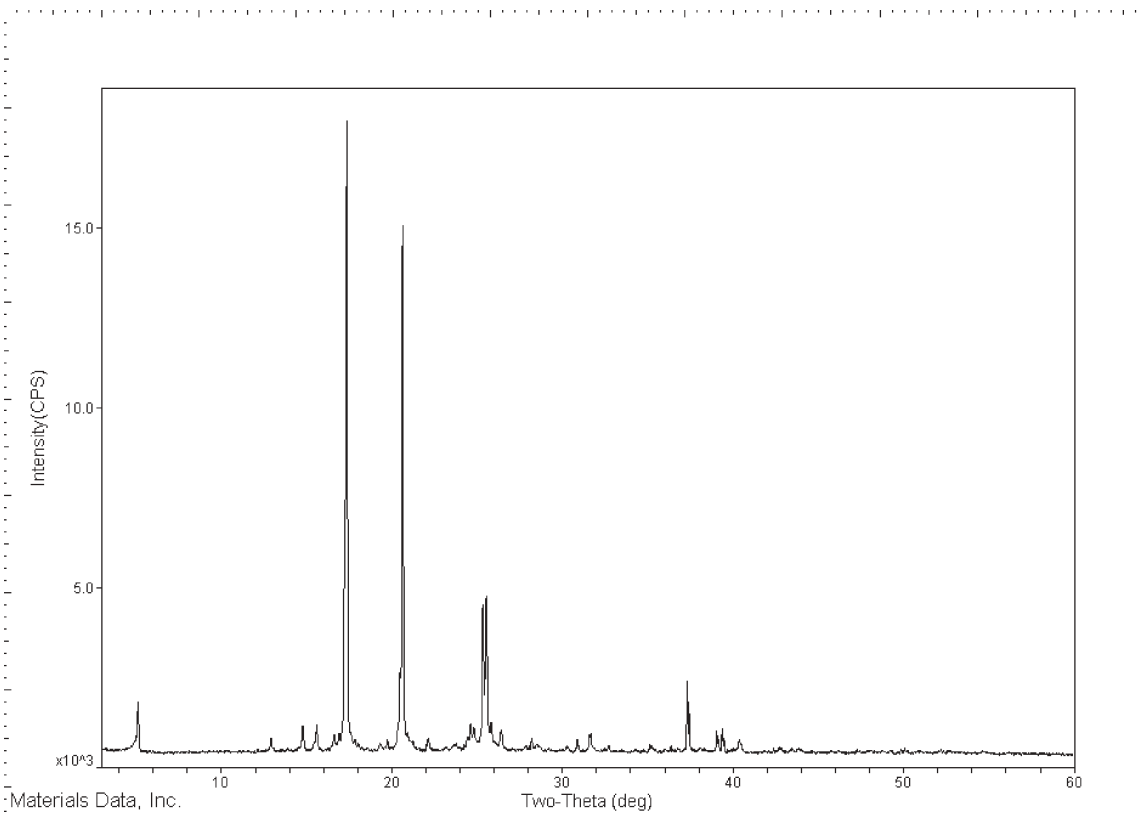

Fig. 3 The powder X-ray pattern of complex **1**.

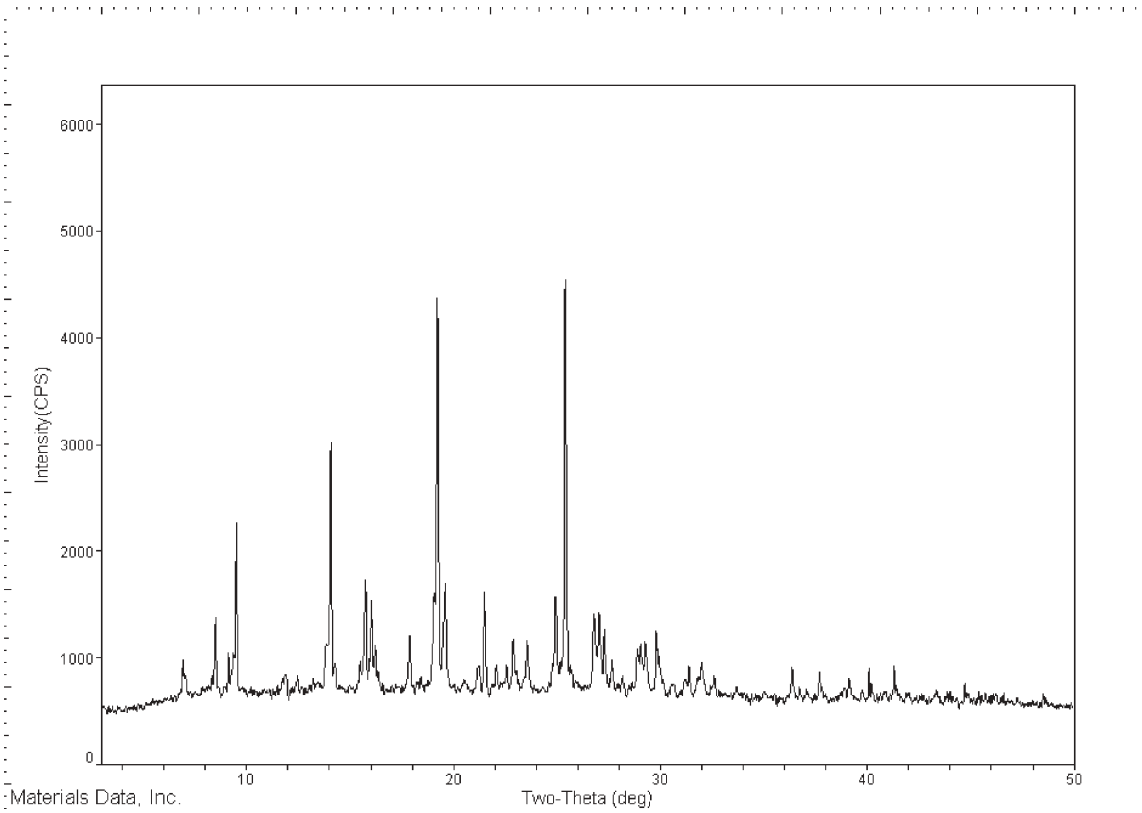

Fig. 4 The powder X-ray pattern of complex **2**.

(**4**), [Mn(4,4′-bipy)$_2$(H$_2$O)$_4$][Cr(C$_2$O$_4$)$_2$(phen)] (**5**), [Mn(4,4′-bipy)$_2$(H$_2$O)$_4$](C$_7$H$_6$NO$_2$)Br(H$_2$O) (**6**), and [Mn(4,4′-bipy)$_2$-(H$_2$O)$_4$][Mn(4,4′-bipy)$_4$(EtOH)$_2$][W$_2$(S)$_4$(C$_4$N$_2$S$_2$)$_2$(4,4′-bipy)(CH$_3$OH) (**7**).[31] The geometries of Mn atoms in these six complexes **1**, **2**, and **4–7** are similar. We can also find totally six complexes with [Mn(4,4′-bipy)(H$_2$O)$_4$] motifs (Mn : 4,4′-bipy = 1 : 1) but receiving polymeric subunits where 4,4′-bipy ligands act as bridging linker.[32–34] Although bond lengths of Mn–O and Mn–N in complexes **1**, **2**, and **4–7** are slightly different, all Mn–O and Mn–N bond distances are normal and in the range reported in Mn-4,4′-bipy complexes with [Mn(4,4′-bipy)(H$_2$O)$_4$] subunit.

The structure of complex **3** is based on 1-D polymer, where each Mn centre is in an octahedral geometry defined by three oxygen atoms from three water molecules, one nitrogen donor from one 4,4′-bipyridine, and two oxygen atoms, one from a sulfonyl and one from a carboxyl group of two different sb ligands (Fig. 7). The powder X-ray pattern is shown in Fig. 8, which is in good accordance with the simulated pattern made on the basis of the CIF using the Mercury program (Fig. 9). In

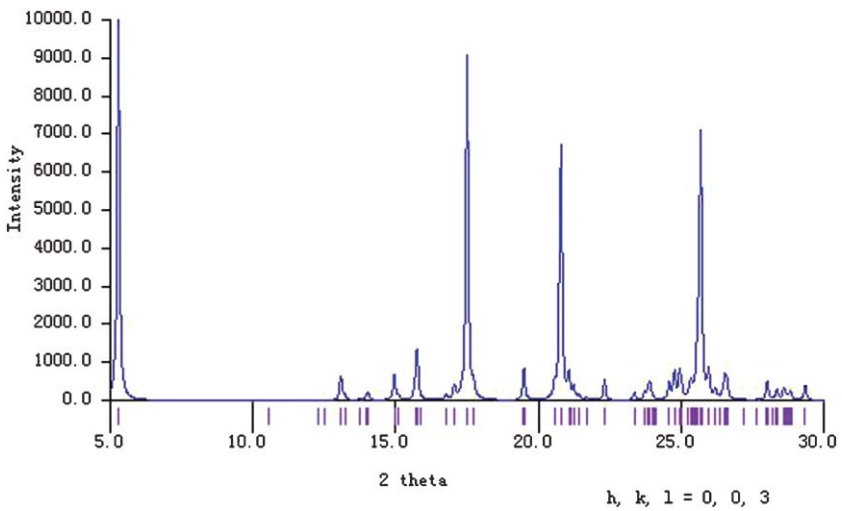

Fig. 5 The simulated X-ray pattern of complex **1** derived by Mercury from CIF.

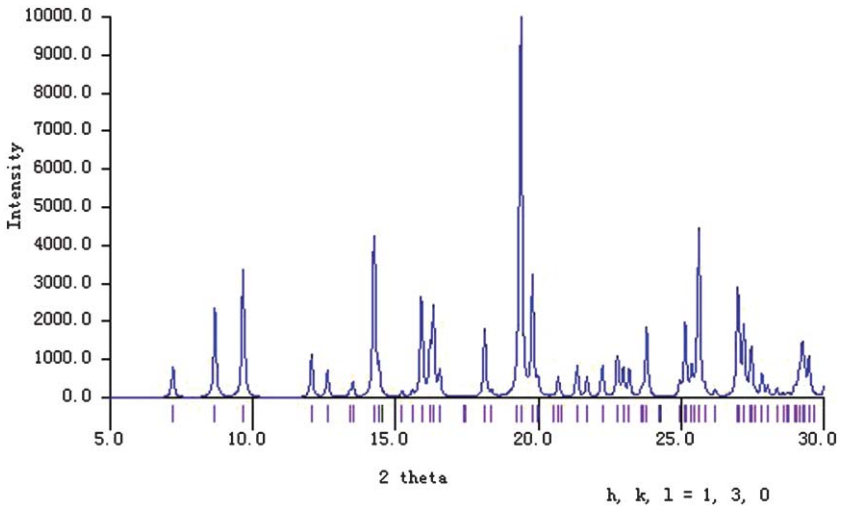

Fig. 6 The simulated X-ray pattern of complex **2** derived by Mercury from CIF.

Table 2 Selected bond lengths (Å) and angles (°) for complex **1**

Mn1–O1	2.182(3)	Mn1–O2	2.199(3)
Mn1–N1	2.250(3)	S1–O5	1.446(3)
S1–O6	1.438(4)	S1–O7	1.446(3)
O1–Mn1–O2	88.36(11)	O1–Mn1–O2^{i}	91.64(11)
O1–Mn1–N1	93.10(10)	O1^{i}–Mn1–N1	86.87(10)
O2–Mn1–N1	91.13(13)	O2^{i}–Mn1–N1	88.87(13)
O5–S1–O6	111.1(2)	O5–S1–O7	111.1(2)
O6–S1–O7	114.9(3)		

[a] Symmetry code, i: $-x + 2, -y + 2, 1 - z$.

contrast to the free forms in **1** and **2**, the sb in **3** is bis-monodentate-coordinated to Mn atoms, resulting in a 1-D polymer (Fig. 10) with the separation Mn···Mn by sb being 10.145(1) Å. The observed Mn–N bond distances in **3** are close to those in **2** whereas the Mn–O distances except Mn1–O1 are close to those in **1**. Further, compared to the dihedral angles between carboxylates and benzene rings in complexes **1** and **2** [6.8(9) and 8.8(2)°, respectively], an increase of the twist angle between the carboxylate and its attached ring [9.2(5)°] is due to the coordination of the carboxylate and the sulfonyl in **3**.

The coordination mode of all 4,4′-bipy ligands in these three complexes is monodentate, therefore the structures of complexes **1** and **2** are monomer, whereas complex **3** is a polymeric species due to sb bridging. The dihedral angles between two rings of the 4,4′-bipyridine are 34.7(2)° in **1**, 21.8(1) and 22.0(1)° in **2**, and 29.47(9)° in **3**, respectively, indicating that the dihedral angles in **2** are apparently relatively small, whereas they are still close to those in **1** and **3**. Further, another terminal N donor of each 4,4′-bipy is blocked to coordinate to metal by hydrogen bonding. It is worth noting that in complex **4** the monodentate 4,4′-bipy in the motif of $[Mn(4,4'\text{-bipy})_2(H_2O)_4]$ does not form any hydrogen bond while significant stacking effect with adjacent 4,4′-bipyridine occurs. In all previously reported monodentate 4,4′-bipyridine manganese(II) complexes (totally six including **1** and **2**) except **4** all nitrogen terminal atoms form hydrogen bonds, indicating the hydrogen-bonding interactions are a more popular driving force for the formation of monodentate 4,4′-bipyridine mode.

It should be pointed out that coordinated water molecules, solvated water molecules, and monodentate 4,4′-bipyridine ligands in these three complexes generate extensive hydrogen-bonding interactions. Although complexes **1** and **2** are cation–anion species and share the same cation motifs, these motifs

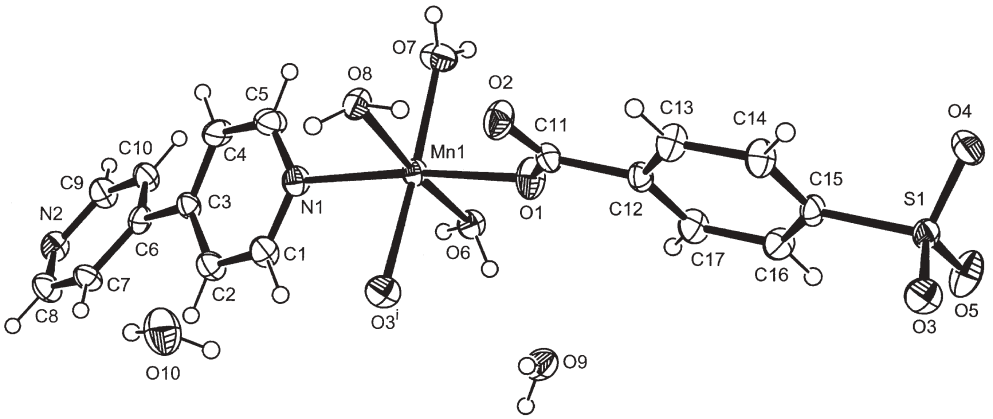

Fig. 7 ORTEP view of a fragment of complex **3**, with 40% probability displacement ellipsoids. [Symmetry code (i): $-x + 3, -y + 1, 2 - z$.]

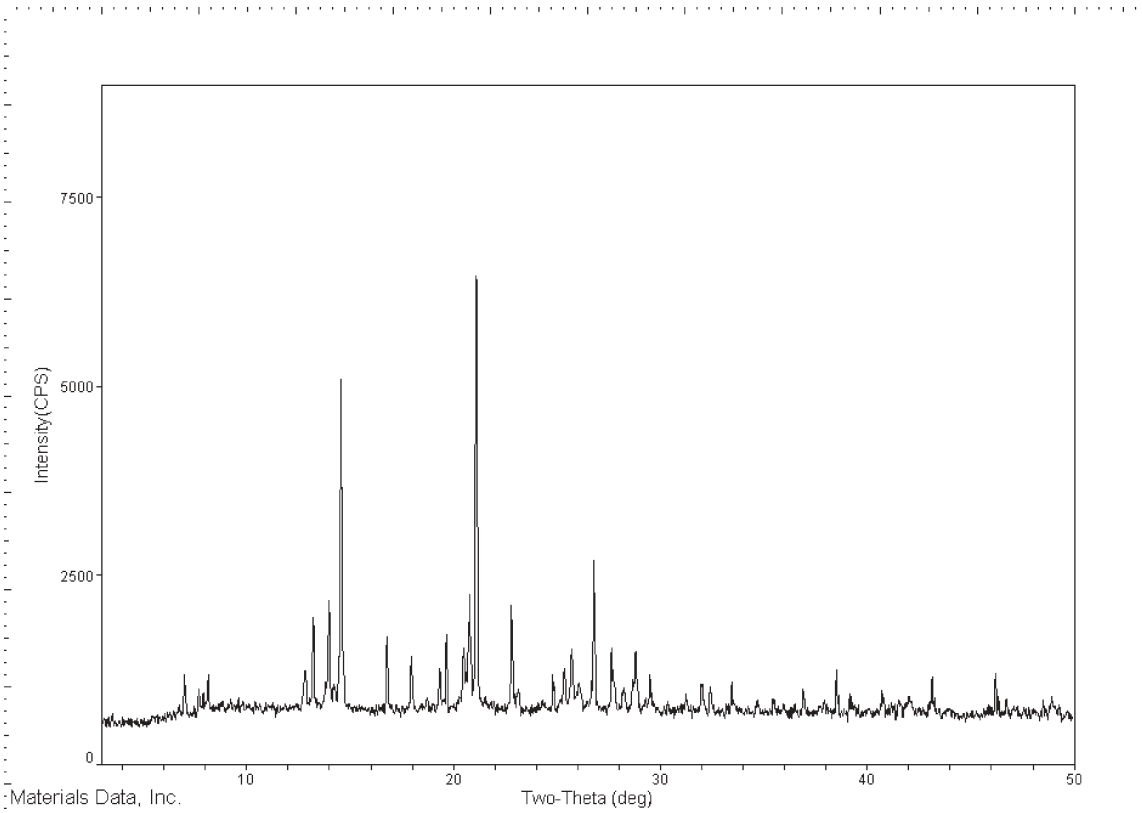

Fig. 8 The powder X-ray pattern of complex **3**.

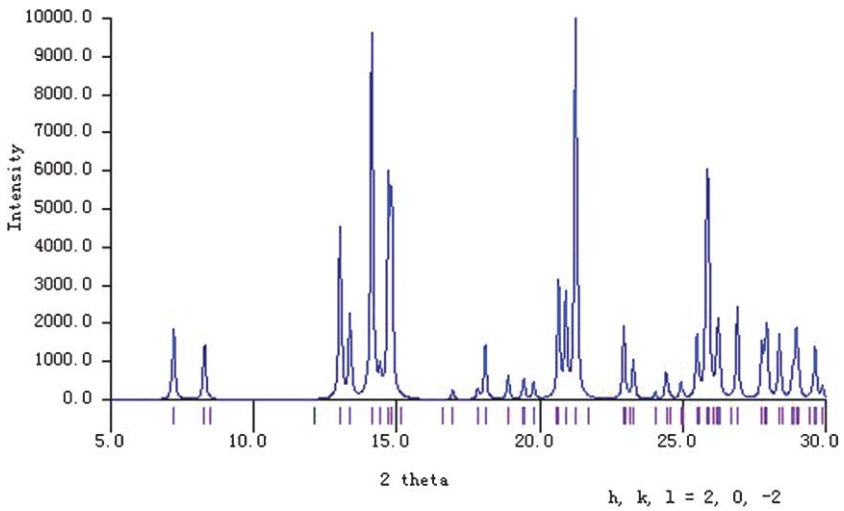

Fig. 9 The simulated X-ray pattern of complex **3** derived by Mercury from CIF.

$[Mn(4,4'\text{-bipy})_2(H_2O)_4]^{2+}$ form very different hydrogen-bonding patterns. In complex **1**, each $[Mn(4,4'\text{-bipy})_2(H_2O)_4]^{2+}$ motif using its uncoordinated N donor forms a hydrogen bond with the carboxyl of the Hsb ligand in N···H–O type, where the sulfonate group of Hsb further forms hydrogen bonding with three cations. Four water molecules in each cation are all associated with hydrogen bonds: O1 and $O1^{i}$ (symmetry code i: $-x + 2, -y + 2, 1 - z$) form two hydrogen bonds with sulfonate groups, respectively, and O2 and $O2^{i}$ form one hydrogen bond with the sulfonate group, respectively. Therefore, each cation forms hydrogen bonds with eight Hsb ligands (Fig. 11 and Table 3). As a result, the gross structure of complex **1** is a 3-D hydrogen-bonding architecture (Fig. 12 and Table 3). In complex **2** (selected bond lengths and angles for complex **2** are given in Table 4) the cation motifs, $[Mn(4,4'\text{-bipy})_2(H_2O)_4]^{2+}$, form 1-D hydrogen-bonding chains (Fig. 13 and Table 5) with the adjacent Mn···Mn separation of 12.4646(9) Å, which is significantly longer than those in

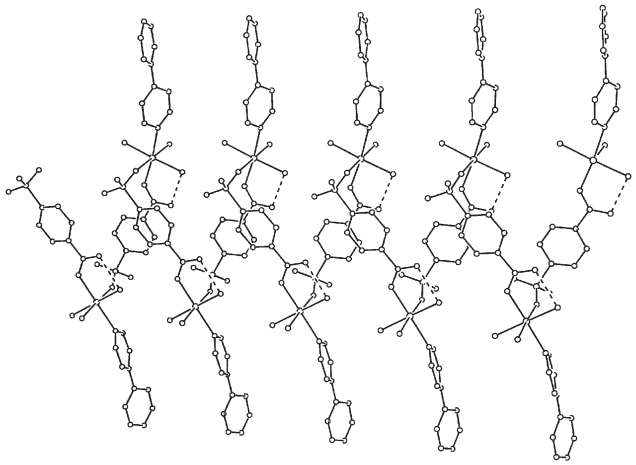

Fig. 10 View of 1-D polymeric chain for complex **3**. H atoms have been omitted for clarity.

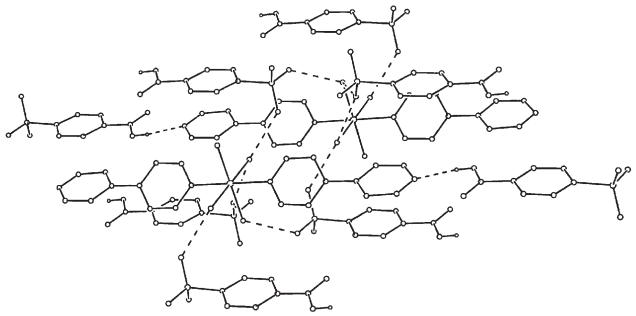

Fig. 11 View of hydrogen bonding pattern in complex **1**.

coordinated bridging 4,4′-bipyridine complexes [about 11.5 Å].[32–34] On the other hand, anions and lattice water molecules form a 2-D hydrogen-bonding layer. Further, such 2-D layers and coordinated water molecules in 1-D cation chains form 3-D architecture (Fig. 14 and Table 5). In the 1-D polymeric complex **3**, there is an intra-hydrogen bonding between the uncoordinated carboxyl oxygen atom and the coordinated water molecule (elected bond lengths and angles for complex **3** are given in Table 6). Moreover, the uncoordinated N atom of the 4,4′-bipyridine, coordinated water molecules, and sulfonate in 1-D chain form hydrogen bonds with lattice water molecules and adjacent 1-D chain, resulting in the 3-D extended hydrogen-bonding supramolecular architecture (Fig. 15 and Table 7).†

As reported, there are extensive stacking effects found in 4,4′-bipyridine complexes.[35] In complex **1**, however, there is no any significant π–π stacking effect. In complex **2**, in the 1-D cation hydrogen-bonding polymer exist significantly stacking interactions between 4,4′-bipyridine ligands and the centroid to centroid distances between pyridyl rings are about 3.68 Å, while there is no significantly stacking interaction between chains or between 4,4′-bipy and sb or between sb ligands. In complex **3**, stacking effect also only exists between

† CCDC reference numbers 602728–602730. For crystallographic data in CIF or other electronic format see DOI: 10.1039/b611300a

Table 3 Hydrogen-bonding geometry parameters (Å,°) for complex **1**

D–H···A	D–H	H···A	D···A	D–H···A
O3–H3···N2^{i}	0.82	1.99	2.794(7)	165.7
O1–H1A···O5^{ii}	0.84(4)	1.89(4)	2.727(4)	171(5)
O1–H1B···O6^{iii}	0.84(4)	1.97(2)	2.769(4)	156(5)
O2–H2A···O6^{iii}	0.84(3)	2.41(3)	3.068(5)	135(4)
O2–H2B···O7^{iv}	0.84(4)	1.90(4)	2.738(4)	175(5)

[a] Symmetry codes, i: $-x+3, -y+1, -z+2$; ii: $x+1, y, z$; iii: $-x+2, -y+2, -z+1$; iv: $-x+2, -y+1, -z+1$.

4,4′-bipyridine ligands with the centroid to centroid distance of 3.719(2) Å.

Ligands in above three complexes display simple coordination modes, monodentate function for 4,4′-bipyridine and free or bis-dentate mode for sb. In the lead complex, sb exhibits multiple coordination modes,[36] while in manganese complexes with 2,2′-bipyridine or 1,10-phenanthroline ligands recently synthesized in our lab,[37] the sb also displays simple mode. Interestingly, the three topologically diverse structures based on Mn^{2+}/sb/4,4′-bipyridine system only display monodentate function for all 4,4′-bipyridine ligands, which is the first example that the monodentate function of the 4,4′-bipyridine ligand systematically occurs in a series of compounds within the same system.

Comparison between bdc with two carboxylate groups and sb with one carboxylate and one sulfonate may give us some valuable information. All bdc/4,4′-bipyridine complexes do not show the monodentate function for 4,4′-bipyridine, probably suggesting the sulfonate has weaker coordination ability than that of the carboxyl group, therefore the coordination ability between the sb and 4,4′-bipyridine ligands is close, which suggests that the coordination mode of 4,4′-bipyridine largely depends on synthesis conditions whereas in the case of bdc/4,4′-bipyridine it is reasonable that the carboxylates are overwhelmingly coordinated to metal atoms due to strong coordination ability of the carboxylate, then the 4,4′-bipy ligand either coordinates the remaining vacant sites in bridging mode or acts as a free ligand.

It is noteworthy that two rings of each monodentate 4,4′-bipy are significantly non-planar whereas in the bridging mode, some of them are coplanar, indicating that the monodenate 4,4′-bipyridine is more flexible than that in bridging, therefore uncoordinated N donor has a larger thermal motion than that of coordinated N atom although the uncoordinated N atom is hydrogen-bonded or stacked.

In the field of crystal engineering, the pyridine–carboxylic acid motif has been used as an important supramolecular synthon.[38] Our investigation also provides an interesting supramolecular synthon to expand novel supramolecular architecture through coordination and hydrogen bonding by monodentate 4,4′-bipyridine ligand.

Exclusion of water and monodentate 4,4′-bipyridine molecules

Thermogravimetric analyses (TGA) have been performed on complexes **1–3** by heating each complex to 800 °C. TGA for **1** showed the loss of about two water molecules in the range 98–110 °C (calculated 4.3%, observed 4.6%), followed by a plateau in the range 121–156 °C, then the sample lost weight again in

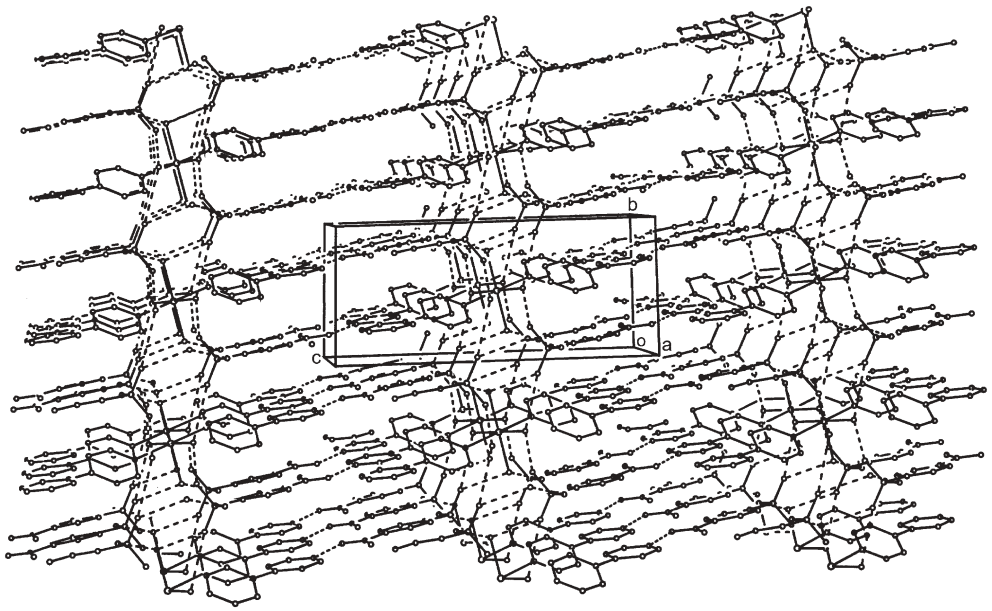

Fig. 12 The 3-D hydrogen-bonding network of complex **1**.

Table 4 Selected bond lengths (Å) and angles (°) for complex **2**

Mn1–O6	2.159(3)	Mn1–O7	2.159(3)
Mn1–O8	2.152(3)	Mn1–O9	2.196(3)
Mn1–N1	2.270(3)	Mn1–N3	2.285(3)
S1–O3	1.448(3)	S1–O4	1.447(3)
S1–O5	1.438(3)		
O8–Mn1–O6	178.76(17)	O8–Mn1–O7	89.36(14)
O6–Mn1–O7	91.55(14)	O8–Mn1–O9	92.66(14)
O6–Mn1–O9	86.42(15)	O7–Mn1–O9	177.24(15)
O6–Mn1–N1	91.20(12)	O7–Mn1–N1	89.61(15)
O8–Mn1–N1	87.95(13)	O9–Mn1–N1	88.58(15)
O6–Mn1–N3	90.57(12)	O7–Mn1–N3	91.83(14)
O8–Mn1–N3	90.25(12)	O9–Mn1–N3	90.05(15)
N1–Mn1–N3	177.69(17)	O4–S1–O3	112.8(2)
O5–S1–O3	112.7(2)	O5–S1–O4	112.1(2)

the range 156–262 °C. The overall weight loss in the range 98–262 °C is 43.9%, corresponding to the removal of four water molecules and two 4,4′-bipyridine ligands (calculated 45.6%). TGA for **2** shows that eight water molecules were lost in the temperature range 69–132 °C (calculated 20.3%. observed 19.1%), then followed by the loss of two 4,4′-bipyridine ligands in the range 132–461 °C. The sum of weight loss in the range 69–461 °C is 62.4%, corresponding to the removal of eight water molecules and two 4,4′-bipyridine ligands (calculated 64.1%). TGA for **3** showed that the first loss took place between 97–161 °C, corresponding to the removal of five water molecules (calculated 18.0%, observed 16.3%), then followed by the loss of 4,4′-bipyridine ligand above 206 °C. Totally, the weight loss in the range 97–398 °C is 48.2%, corresponding to the release of five water molecules and one 4,4′-bipyridine ligand (calculated 49.1%).

Emission properties

An obvious feature is that complexes **1–3** display strong blue emissions at 413, 452, and 469 nm for **1**, at 424, 453, and 471 nm for **2**, and at 453 and 470 nm for **3** in solid state at room temperature. The maximal peaks occur at 469, 424, and 470 nm for complexes **1–3**, respectively. These emissions come from 4,4′-bipyridine and 4-sulfobenzoate ligands[39] and are probably neither metal-to-ligand nor ligand-to-metal charge transfer. It is worth noting that the fluorescent intensity of **3** is significantly stronger than those in **1** and **2**, which is largely contributed to the enhancement of the coordinated 4-sulfobenzoate or ligand-to-ligand.

Conclusion

In summary, three complexes assembled by manganese(II) salts, 4-sulfobenzoate, and 4,4′-bipyridine have been synthesized and characterized. The most interesting topological feature in complexes **1–3** is the monodentate function for 4,4′-bipyridine. As to references, such complexes were occasionally obtained in separate systems, while the introduction of 4-sulfobenzoate ligand combined with manganese(II) salt systematically leads to the coordination of monodentate 4,4′-bipyridine. Basically, the sulfonate group is weaker in coordination ability than that of the carboxylate group, while

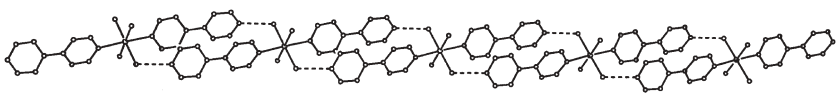

Fig. 13 The 1-D hydrogen-bonding pattern of cations in complex **2**. Hydrogen bonds are shown as dashed lines.

Table 5 Hydrogen-bonding geometry parameters (Å,°) for complex **2**

D–H···A	D–H	H···A	D···A	D–H···A
O6–H6B···O10^{i}	0.86(4)	1.99(4)	2.825(5)	165(4)
O8–H8A···O3^{ii}	0.85(5)	1.99(5)	2.798(4)	162(5)
O6–H6A···N2^{iii}	0.85(3)	1.89(3)	2.739(5)	177(5)
O8–H8B···N4^{iv}	0.85(3)	1.97(3)	2.809(5)	169(4)
O7–H7B···O1^{i}	0.85(3)	1.85(3)	2.686(5)	167(5)
O7–H7B···O10^{v}	0.85(3)	1.91(3)	2.762(5)	178(5)
O9–H9A···O11	0.85(3)	1.84(3)	2.680(6)	168(5)
O9–H9B···O3^{vi}	0.85(3)	2.12(3)	2.941(5)	163(5)
O12–H12A···O5	0.85(3)	1.91(3)	2.749(5)	174(5)
O12–H12B···O11^{vii}	0.85(1)	2.11(2)	2.906(5)	156(5)
O11–H11A···O13	0.86(3)	1.78(4)	2.622(7)	166(5)
O11–H11B···O4^{ii}	0.85(3)	2.03(3)	2.857(5)	167(6)
O13–H13A···O1^{viii}	0.86(3)	1.82(2)	2.639(5)	160(5)
O10–H10A···O12^{ix}	0.85(3)	1.96(3)	2.809(5)	174(5)
O10–H10B···O2	0.86(4)	1.92(4)	2.762(5)	170(4)

[a] Symmetry codes, i: $x+1, y, z+1$; ii: $-x, y-1/2, -z$; iii: $x, y, z+1$; iv: $x, y, z-1$; v: $x+2, y, z+1$; vi: $-x-1, y-1/2, -z$; vii: $-x-1, y+1/2, -z$; viii: $-x-1, y-1/2, -z-1$; ix: $x-1, y, z-1$.

in complexes **1–3** the sulfonate can mediate or balance the competition ability or the coordination ability between the 4,4′-bipyridine and carboxylate, thus weak interactions, such as hydrogen bonds or stacking interactions play an important role in the assembly of molecular structures. Therefore, hydrogen bonding can unexpectedly but systematically block the metal–metal bridging by 4,4′-bipyridine in complexes **1–3**. Successful exploration in these three complexes may provide useful information for other combination systems with 4,4′-bipyridine to control the coordination ability of bridging ligands and construct novel functional frameworks with specific topologies.

Table 6 Selected bond lengths (Å) and angles (°) for complex **3**

Mn1–O1	2.127(2)	Mn1–O3^{i}	2.192(2)
Mn1–O6	2.191(2)	Mn1–O7	2.167(2)
Mn1–O8	2.213(3)	Mn1–N1	2.294(3)
S1–O3	1.459(2)	S1–O4	1.455(2)
S1–O5	1.439(3)		
O1–Mn1–O3^{i}	87.62(10)	O1–Mn1–O6	88.97(10)
O1–Mn1–O7	94.79(11)	O1–Mn1–O8	90.60(10)
O1–Mn1–N1	173.70(11)	O6–Mn1–O3^{i}	95.04(10)
O7–Mn1–O3^{i}	177.17(13)	O3^{i}–Mn1–O8	90.36(10)
O3^{i}–Mn1–N1	87.46(9)	O7–Mn1–O6	86.50(10)
O6–Mn1–O8	174.56(9)	O6–Mn1–N1	87.56(10)
O7–Mn1–O8	88.14(10)	O7–Mn1–N1	90.24(11)
O8–Mn1–N1	93.36(10)	O4–S1–O3	109.89(15)
O5–S1–O3	113.08(18)	O5–S1–O4	113.6(2)

[a] Symmetry code, i: $3-x, 1-y, 2-z$.

Acknowledgements

The authors thank the Qufu Normal University and Wenzhou Normal College for the diffraction measurements, the National Natural Science Foundation of China (Grant No. 50073019), and the Analytical and Measurement Fund of Zhejiang Province.

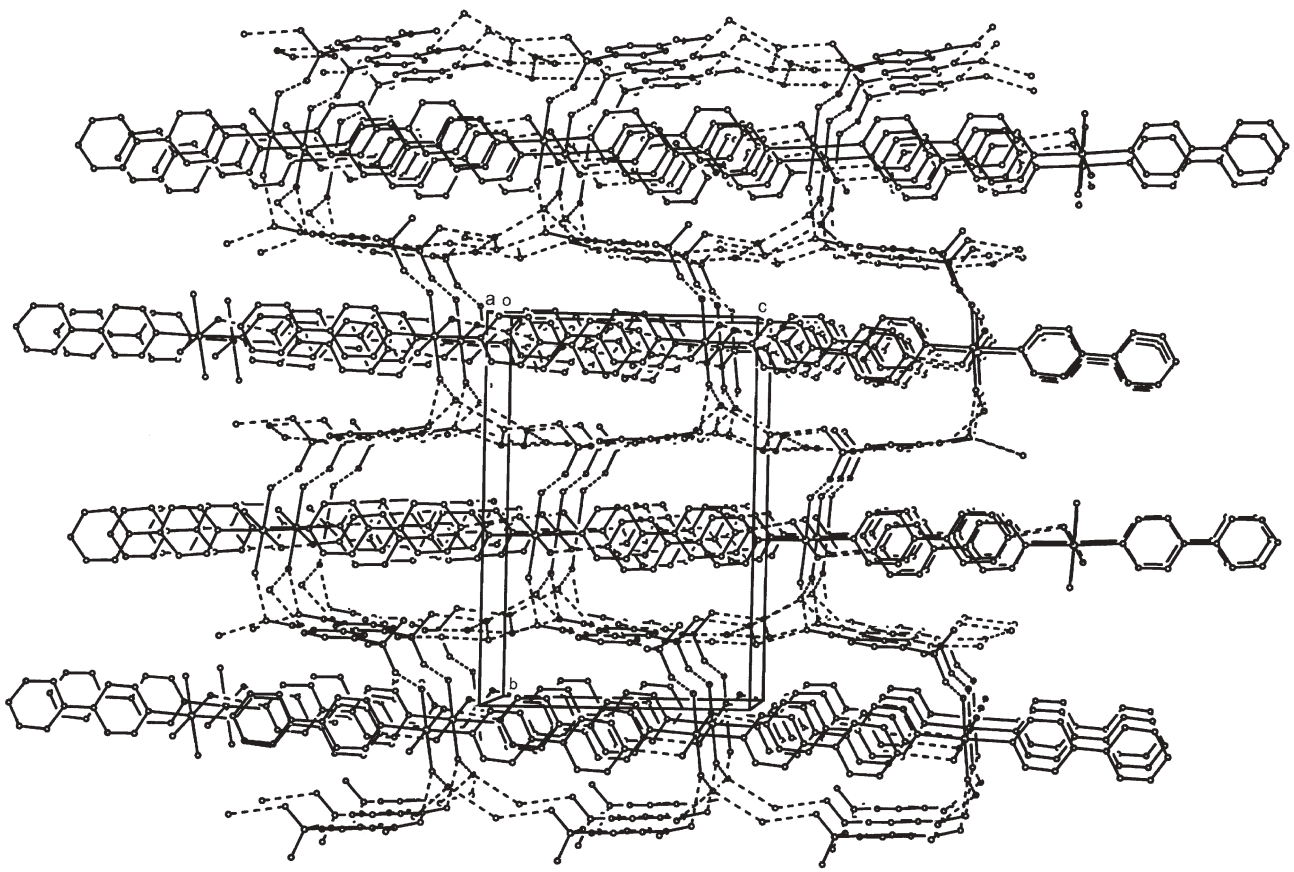

Fig. 14 The 3-D hydrogen-bonding network of complex **2**.

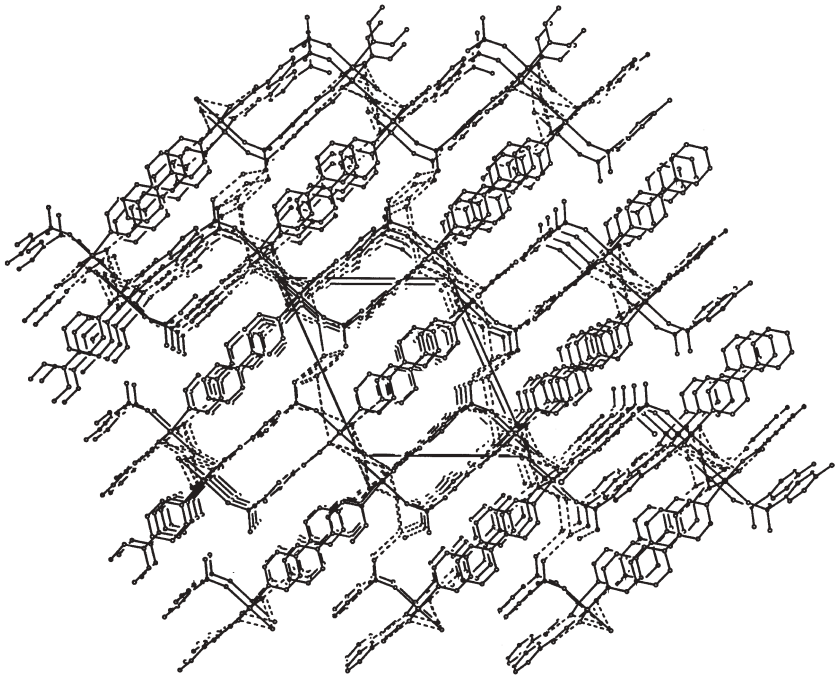

Fig. 15 The 3-D hydrogen-bonding network for complex **3**.

Table 7 Hydrogen-bonding geometry parameters (Å,°) for complex **3**

D–H···A	D–H	H···A	D···A	D–H···A
O6– H6A···N2^{i}	0.86(3)	1.84(3)	2.692(3)	177(6)
O6– H6B···O9	0.85(4)	1.86(4)	2.708(4)	173(6)
O7–H7A···O6^{ii}	0.84(4)	1.99(2)	2.792(4)	158(4)
O7–H7B···O8^{iii}	0.85(4)	1.93(5)	2.768(4)	169(5)
O8–H8B···O1	0.85(3)	2.63(5)	3.085(4)	115(4)
O8–H8A···O2	0.85(3)	1.72(4)	2.559(3)	171(5)
O8–H8A···O9^{iv}	0.86(4)	1.95(4)	2.779(4)	162(4)
O9–H9B···O5^{v}	0.85(5)	1.96(5)	2.777(4)	162(4)
O9–H9B···O10^{vi}	0.85(3)	1.94(4)	2.770(4)	168(5)
O10–H10A···O4^{vii}	0.85(3)	2.06(4)	2.868(4)	159(4)
O10–H10B···O4^{viii}	0.85(2)	2.26(2)	3.037(5)	152(5)

[a] Symmetry codes, i: $-x+1, y+1/2, -z+1$; ii: $-x+2, y-1/2, -z+2$; iii: $-x+2, y+1/2, -z+2$; iv: $x, y-1, z$; v: $-x+3, y-1/2, -z+2$; vi: $x, y+1, z$; vii: $x-1, y-1, z-1$; viii: $-x+3, y-1/2, -z+2$.

References

1 (*a*) S. Kitagawa, R. Kitaura and S. Noro, *Angew. Chem., Int. Ed.*, 2004, **43**, 2334; (*b*) S. Noro, R. Kitaura, M. Kondo, S. Kitagawa, T. Ishii, H. Matsuzaka and M. Yamashita, *J. Am. Chem. Soc.*, 2002, **124**, 2568; (*c*) S. Kitagawa and M. Kondo, *Bull. Chem. Soc. Jpn.*, 1998, **71**, 1739; (*d*) C. Janiak, *Dalton Trans.*, 2003, 2781; (*e*) S. L. James, *Chem. Soc. Rev.*, 2003, **32**, 276.

2 (*a*) N. L. Rosi, J. Eckert, M. Eddaoudi, D. T. Vodak, J. Kim, M. O'Keeffe and O. M. Yaghi, *Science*, 2003, **300**, 1127; (*b*) O. M. Yaghi, M. O'Keeffe, N. W. Ockwig, H. K. Chae, M. Eddaoudi and J. Kim, *Nature*, 2003, **423**, 705; (*c*) M. Eddaoudi, D. B. Moler, H. L. Li, B. L. Chen, T. M. Reineke, M. O'Keeffe and O. M. Yaghi, *Acc. Chem. Res.*, 2001, **34**, 319; (*d*) O. M. Yaghi, H. L. Li, C. Davis, D. Richardson and T. L. Groy, *Acc. Chem. Res.*, 1998, **31**, 474; (*e*) S. L. Zheng and X. M. Chen, *Aust. J. Chem.*, 2004, **57**, 703; (*f*) D. Maspoch, D. Ruiz-Molina and J. Veciana, *J. Mater. Chem.*, 2004, **14**, 2713; (*g*) S. R. Batten and K. S. Murray, *Coord. Chem. Rev.*, 2003, **246**, 103.

3 (*a*) H. Abourahma, G. J. Bodwell, J. J. Lu, B. Moulton, I. R. Pottie, R. B. Walsh and M. J. Zaworotko, *Cryst. Growth Des.*, 2003, **3**, 513; (*b*) H. Abourahma, G. J. McManus, B. Moulton, R. B. Walsh and M. J. Zaworotko, *Macromol. Symp.*, 2003, **196**, 213; (*c*) B. Moulton and M. J. Zaworotko, *Chem. Rev.*, 2001, **101**, 1629; (*d*) L. Carlucci, G. Ciani and D. Proserpio, *Coord. Chem. Rev.*, 2003, **246**, 247.

4 (*a*) N. J. Burke, A. D. Burrows, M. F. Mahon and L. S. Pritchard, *CrystEngComm*, 2003, **5**, 355; (*b*) A. D. Burrows, K. Cassar, R. M. W. Friend, S. P. Rigby and J. E. Warren, *CrystEngComm*, 2005, **7**, 548.

5 (*a*) L. G. Zhu, H. P. Xiao and J. Y. Lu, *Inorg. Chem. Commun.*, 2004, **7**, 94; (*b*) L. G. Zhu, A. Q. Ma and J. Y. Lu, *Inorg. Chem. Commun.*, 2004, **7**, 1053; (*c*) A. Q. Ma and L. G. Zhu, *Inorg. Chem. Commun.*, 2004, **7**, 186; (*d*) A. Q. Ma, Z. Shi, R. R. Xu, W. Q. Pang and L. G. Zhu, *Chem. Lett.*, 2003, **32**, 1010.

6 (*a*) M. D. Hollingsworth, *Science*, 2002, **295**, 2410; (*b*) B. Kesanli and W. B. Lin, *Coord. Chem. Rev.*, 2003, **246**, 305; (*c*) J. Y. Lu, *Coord. Chem. Rev.*, 2003, **246**, 327; (*d*) D. Braga, *Chem. Commun.*, 2003, 2751.

7 M. Eddaoudi, J. Kim, N. Rosi, D. Vodak, J. Wachter, M. O'Keeffe and O. M. Yaghi, *Science*, 2002, **295**, 469.

8 L. P. Zhang and L. G. Zhu, *Acta Crystallogr., Sect. E: Struct. Rep. Online*, 2005, **61**, m1768.

9 S. Martin, M. G. Barandika, L. Lezama, J. L. Pizarro, Z. E. Serna, J. I. Larramendi, M. I. Arriortua, T. Rojo and R. Cortes, *Inorg. Chem.*, 2001, **40**, 4109.

10 (*a*) S. Noro, S. Kitagawa, M. Kondo and K. Seki, *Angew. Chem., Int. Ed.*, 2000, **39**, 2082; (*b*) M. Kondo, T. Okubo, A. Asami, S. Noro, T. Yoshitomi, S. Kitagawa, T. Ishii, H. Matsuzaka and K. Seki, *Angew. Chem., Int. Ed.*, 1999, **38**, 140.

11 C. Z. Lu, C. D. Wu, H. H. Zhuang and J. S. Huang, *Chem. Mater.*, 2002, **14**, 2649.

12 E. J. Cussen, J. B. Claridge, M. J. Rosseinsky and C. J. Kepert, *J. Am. Chem. Soc.*, 2002, **124**, 9574.

13 A. J. Fletcher, E. J. Cussen, T. J. Prior, M. J. Rosseinsky, C. J. Kepert and K. M. Thomas, *J. Am. Chem. Soc.*, 2001, **123**, 10001.

14 E. Suresh, K. Boopalan, R. V. Jasra and M. Bhadhade, *Inorg. Chem.*, 2001, **40**, 4078.

15 L. G. Zhu and S. Kitagawa, *Inorg. Chem. Commun.*, 2003, **6**, 1051.

16 H. Y. He, L. G. Zhu and S. W. Ng, *Acta Crystallogr., Sect. E: Struct. Rep. Online*, 2005, **61**, m601.

17 M. X. Li, H. Z. Liu, Z. Xu and Y. Z. You, *J. Fudan Univ. (Nat. Sci.)*, 1995, **34**, 19.

18 K. R. Leopold and A. Haim, *Inorg. Chem.*, 1978, **17**, 1753.

19 K. Abu-Shandi, C. Janiak and B. Kersting, *Acta Crystallogr., Sect. C: Cryst. Struct. Commun.*, 2001, **57**, 1261.
20 R. F. Klevtsova, L. A. Glinskaya, E. I. Berus and S. V. Larionov, *J. Struct. Chem.*, 2001, **42**, 639.
21 A. S. Attia and C. G. Pierpont, *Inorg. Chem.*, 1995, **34**, 1172.
22 M. Julve, M. Verdaguer, J. Faus, F. Tinti, J. Moratal, A. Monge and E. Gutierrez-Puebla, *Inorg. Chem.*, 1987, **26**, 3520.
23 H. J. Chen, L. Z. Zhang, Z. G. Cai, G. Yang and X. M. Chen, *J. Chem. Soc., Dalton Trans.*, 2000, 2463.
24 Y. C. Jiang, Y. C. Lai, S. L. Wang and K. H. Lii, *Inorg. Chem.*, 2001, **40**, 5320.
25 P. Martiz-Zarza, P. Gili, E. V. Rodriguez-Romero, C. Ruiz-Perez and X. Solans, *Polyhedron*, 1995, **14**, 2907.
26 A. J. Blake, S. J. Hill, P. Hubberstey and W. S. Li, *J. Chem. Soc., Dalton Trans.*, 1997, 913.
27 G. M. Sheldrick, SADABS, Program for Bruck Area Detector Absorption Correction, University of Göttingen, Germany, 1997.
28 G. M. Sheldrick, SHELXL-97, Program for Crystal Structure Refinement, Göttingen University, 1997.
29 L. J. Farrugia, WinGX-A Windows Program for Crystal Structure Analysis, *J. Appl. Crystallogr.*, 1999, **32**, 837.
30 J. Metz, O. Schenider and M. Hanack, *Spectrochim. Acta, Part A*, 1982, **38A**, 1265.
31 (*a*) M. L. Tong, H. K. Lee, X. M. Chen, R. B. Huang and T. C. W. Mak, *J. Chem. Soc., Dalton Trans.*, 1999, 3657; (*b*) G. Marinescu, M. Andruh, M. Julve, F. Lloret, R. Llusar, S. Uriel and J. Vaissermann, *Cryst. Growth Des.*, 2005, **5**, 261; (*c*) R. H. Wang, F. L. Jiang, Y. F. Zhou, L. Han and M. C. Hong, *Inorg. Chim. Acta*, 2005, **358**, 545; (*d*) S. F. Lu, Y. B. Zhu, Y. C. Liang, R. M. Yu, X. Y. Huang, F. X. Sun, Q. J. Wu and Z. X. Huang, *Acta Chim. Sinica*, 2004, **62**, 253.
32 (*a*) Y. H. Wang, L. Y. Feng, Y. G. Li, C. W. Hu, E. B. Wang, N. H. Hu and H. Q. Jia, *Inorg. Chem.*, 2002, **41**, 6351; (*b*) E. B. Ying, Y. Q. Zheng and H. J. Zhang, *J. Coord. Chem.*, 2004, **57**, 459.
33 (*a*) R. H. Wang, L. H. Chen, M. C. Hong, J. H. Luo, R. Cao and J. B. Weng, *Chin. J. Struct. Chem.*, 2003, **22**, 50; (*b*) S. Gao, L. H. Huo and S. W. Ng, *Acta Crystallogr., Sect. E: Struct. Rep. Online*, 2005, **61**, m2270.
34 S. Sain, T. K. Maji and N. R. Chaudhuri, *Transit. Met. Chem.*, 2002, **27**, 716.
35 H. W. Roesky and M. Andruh, *Coord. Chem. Rev.*, 2003, **236**, 91.
36 L. P. Zhang, L. G. Zhu and H. P. Xiao, *Acta Crystallogr., Sect. E: Struct. Rep. Online*, 2005, **61**, m860.
37 (*a*) L. P. Zhang, L. G. Zhu and H. P. Xiao, *Acta Crystallogr., Sect. E: Struct. Rep. Online*, 2005, **61**, m705; (*b*) L. P. Zhang and L. G. Zhu, *Acta Crystallogr., Sect. E: Struct. Rep. Online*, 2005, **61**, m1036; (*c*) L. P. Zhang, L. G. Zhu and G. Q. Cai, *Acta Crystallogr., Sect. E: Struct. Rep. Online*, 2005, **61**, m2634.
38 B. H. Ye, M. L. Tong and X. M. Chen, *Coord. Chem. Rev.*, 2005, **249**, 545.
39 R. X. Yuan, R. G. Xiong, Y. L. Xie, X. Z. You, S. M. Peng and G. H. Lee, *Inorg. Chem. Commun.*, 2001, **4**, 384.

